

## Preclinical studies on [<sup>11</sup>C]MPDX for mapping adenosine A<sub>1</sub> receptors by positron emission tomography

Kiichi ISHIWATA,\* Tadashi NARIAI,\*\* Yuichi KIMURA,\* Keiichi ODA,\* Kazunori KAWAMURA,\*  
Kenji ISHII,\* Michio SENDA,\*<sup>1</sup> Shinichi WAKABAYASHI\*\*<sup>2</sup> and Junichi SHIMADA\*\*\*

\*Positron Medical Center, Tokyo Metropolitan Institute of Gerontology

\*\*Department of Neurosurgery, Tokyo Medical and Dental University

\*\*\*Pharmaceutical Research Institute, Kyowa Hakko Kogyo Co., Ltd.

In previous *in vivo* studies with mice, rats and cats, we have demonstrated that [<sup>11</sup>C]MPDX ([1-methyl-<sup>11</sup>C]8-dicyclopropylmethyl-1-methyl-3-propylxanthine) is a potential radioligand for mapping adenosine A<sub>1</sub> receptors of the brain by positron emission tomography (PET). In the present study, we performed a preclinical study. The radiation absorbed-dose by [<sup>11</sup>C]MPDX in humans estimated from the tissue distribution in mice was low enough for clinical use, and the acute toxicity and mutagenicity of MPDX were not found. The monkey brain was clearly visualized by PET with [<sup>11</sup>C]MPDX. We have concluded that [<sup>11</sup>C]MPDX is suitable for mapping adenosine A<sub>1</sub> receptors in the human brain by PET.

**Key words:** adenosine A<sub>1</sub> receptor, [<sup>11</sup>C]MPDX, central nervous system, positron emission tomography

### INTRODUCTION

ADENOSINE is an endogenous modulator of several physiological functions in the central nervous system (CNS) as well as in peripheral organs. The effects are mediated by at least four subtypes: A<sub>1</sub>, A<sub>2A</sub>, A<sub>2B</sub> and A<sub>3</sub> receptors.<sup>1–6</sup> The adenosine A<sub>1</sub> receptors in the CNS are present both pre- and post-synaptically in many regions, being rich in the hippocampus, cerebral cortex, thalamic nuclei, basal ganglia and the cerebellar cortex in animals<sup>7–9</sup> and humans.<sup>10–13</sup> On pre-synaptic terminals, their main action is to limit the availability of calcium to the excitation-secretion coupling mechanism involved in the exocytotic release of neurotransmitters such as glutamate, acetylcholine, dopamine, 5-hydroxytryptamine and several peptides.<sup>13</sup> Post-synaptically, adenosine A<sub>1</sub> receptors usually

induce hyperpolarization of cells, at least partly by opening potassium channels.<sup>13</sup>

Based on these backgrounds, we have developed three labeled adenosine A<sub>1</sub> receptor ligands; [1-propyl-<sup>11</sup>C]8-dicyclopropylmethyl-1,3-dipropylxanthine ([<sup>11</sup>C]KF15372) and its methyl ([1-methyl-<sup>11</sup>C]8-dicyclopropylmethyl-1-methyl-3-propylxanthine, [<sup>11</sup>C]MPDX, Fig. 1) and ethyl ([1-ethyl-<sup>11</sup>C]8-dicyclopropylmethyl-1-ethyl-3-propylxanthine) derivatives, and have evaluated their *in vivo* properties.<sup>14–18</sup> In the studies with mice, rats and cats,<sup>16,18</sup> [<sup>11</sup>C]MPDX is of choice as a candidate for application to human PET studies because of easy penetration of the blood-brain barrier and the practically high radiochemical yield, although its affinity for adenosine A<sub>1</sub> receptors was slightly weaker: K<sub>i</sub> values were 3.2, 1.7 and 4.2 nM for KF15372, ethyl derivative and MPDX, respectively. In the rats deprived of retinocollicular fibers by eye enucleation, degeneration of the adenosine A<sub>1</sub> receptors in the contralateral superior colliculus was presented by *ex vivo* autoradiography with [<sup>11</sup>C]MPDX.<sup>16,19</sup> We evaluated quantitatively the adenosine A<sub>1</sub> receptors in the cat brain by PET with [<sup>11</sup>C]MPDX,<sup>18</sup> and preliminarily found that the [<sup>11</sup>C]MPDX PET was more sensitive for predicting the fatal ischemic insult than the cerebral blood flow, glucose metabolism or benzodiazepine receptors

Received March 22, 2002, revision accepted May 27, 2002.

Present address: <sup>1</sup>Institute of Biomedical Research and Innovation, Kobe, Japan and <sup>2</sup>Department of Neurosurgery, Kajikawa Hospital, Hiroshima, Japan.

For reprint contact: Kiichi Ishiwata, Ph.D., Positron Medical Center, Tokyo Metropolitan Institute of Gerontology, 1–1 Nakacho, Itabashi-ku, Tokyo 173–0022, JAPAN.

E-mail: ishiwata@pet.tmig.or.jp.

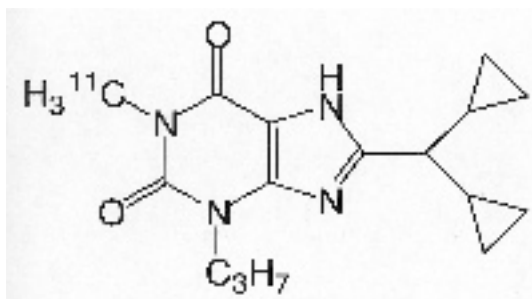


**Fig. 1** Chemical structure of [ $^{11}\text{C}$ ]MPDX.

measured by PET.<sup>20</sup>

In the present study, we calculated the radiation dosimetry of [ $^{11}\text{C}$ ]MPDX for humans from mice data and the acute toxicity and mutagenicity of MPDX in a preclinical study. PET imaging of adenosine  $A_1$  receptors with [ $^{11}\text{C}$ ]MPDX was also performed in the monkey brain.

## MATERIALS AND METHODS

8-Dicyclopropylmethyl-3-propylxanthine and MPDX were synthesized in our laboratory as previously described.<sup>21–23</sup> [ $^{11}\text{C}$ ]MPDX was prepared by methylation of 8-dicyclopropylmethyl-3-propylxanthine with [ $^{11}\text{C}$ ]methyl iodide as described.<sup>16</sup> The specific activity was 18–108 TBq/mmol. Male ddY mice were obtained from Tokyo Laboratory Animals Co., Ltd. (Tokyo, Japan). Rhesus monkeys were transferred from the Institute of Medical Science at the University of Tokyo. The animal studies were approved by the Animal Care and Use Committee of the Tokyo Metropolitan Institute of Gerontology.

### *Tissue distribution in mice*

[ $^{11}\text{C}$ ]MPDX (1.1–2.0 MBq/16–34 pmol) was intravenously injected into mice (8 weeks old). They were killed by cervical dislocation at 1, 5, 15, 30, 60 and 90 min after injection ( $n = 4$ ). The blood was collected by heart puncture, and the tissues were harvested. The samples were measured for the  $^{11}\text{C}$ -radioactivity with an auto-gamma counter and weighed. The tissue uptake of  $^{11}\text{C}$  was expressed as a percentage of the injected dose per organ (%ID/organ) or a percentage of the injected dose per gram of tissue (%ID/g). Based on the tissue distribution data, radiation dosimetry for human adults was estimated by the MIRD method described previously.<sup>24,25</sup>

### *Acute toxicity*

Toxicity studies were performed at the Mitsubishi Chemical Safety Institute Ltd. (Tokyo, Japan). Acute toxicity was assayed in Crj:CD(SD)IGS rats (SPF). MPDX at a dose of 3.73 mg/kg body weight (0.373 mg/ml suspension in physiological saline containing 0.01% Tween 80) was

injected intraperitoneally into 5-week old rats weighing 157–184 g and 129–141 g, for males ( $n = 5$ ) and females ( $n = 5$ ), respectively. The dose of 3.73 mg/kg body weight is the 41000-fold equivalent of the postulated administration dose (0.091  $\mu\text{g}/\text{kg}$  body weight) of 500 MBq [ $^{11}\text{C}$ ]MPDX with a specific activity of 37 TBq/mmol for humans weighing 60 kg. The three lots of [ $^{11}\text{C}$ ]MPDX prepared above were also assayed after decay-out of  $^{11}\text{C}$ . Each of the three [ $^{11}\text{C}$ ]MPDX preparations was injected intravenously into 5-week old male rats ( $n = 5$ ) at doses of 1.4–5.7  $\mu\text{g}/0.77$ –1.5 ml/kg body, which were 40-fold equivalent to the postulated administration dose of [ $^{11}\text{C}$ ]MPDX for humans. One lot (5.7  $\mu\text{g}/1.5$  ml/kg body weight) was also injected into 5-week old female rats ( $n = 5$ ). They were observed four times (0.5, 1, 3 and 6 h after the injection) at day 1 and thereafter once daily for clinical signs until 15 days, and weighed on days 4, 8 and 15. At the end of the 15 day-observation period, the rats were euthanized and a macroscopic analysis was performed.

### *Ames test*

Mutagenicity tests were performed at the Mitsubishi Chemical Safety Institute Ltd. (Tokyo, Japan). MPDX was tested for mutagenicity in the Ames test with four histidine-requiring strains of *Salmonella typhimurium* (TA98, TA100, T1535 and T1537) at a dose range of 0.0763–5000  $\mu\text{g}/\text{plate}$  by the standard method.

### *PET imaging of adenosine $A_1$ receptors in the monkey brain*

The PET camera used was a model SHR 2000 (Hamamatsu Photonics K.K., Hamamatsu, Japan).<sup>26</sup> The camera consists of four-ring detectors and acquires seven slices at a center-to-center interval of 6.5 mm with a resolution of 4.0 mm full width at half maximum in the transaxial plane.

Two female rhesus monkeys (22 and 23 years old, weighing 3.2 kg) were anesthetized with 0.01–0.05% isoflurane, and PET scanning was performed as previously.<sup>17</sup> Catheters were inserted into the femoral vein and femoral artery. [ $^{11}\text{C}$ ]MPDX (91 MBq/4.1 nmol and 141 MBq/5.6 nmol) was injected intravenously into the monkey, and a time sequential tomographic scan was performed in the transverse section of the brain parallel to the orbitomeatal line for 60 min (ten 1-min frames, four 5-min frames and three 10-min frames) as described above. Based on the standard MRI images as prepared previously,<sup>17</sup> regions of interest were placed on the frontal cortex, occipital cortex, parietal cortex, temporal cortex, thalamus, cerebellum and brain stem, and the time-activity curves were obtained. The decay-corrected radioactivity value was expressed as the standardized uptake value [SUV, (regional activity/ml volume)/(injected activity/g body weight)].

Blood was collected from the vein 1, 5, 15, 30 and 60 min after the tracer injection, and the plasma was obtained by centrifugation. The radioactivity level of the plasma

**Table 1** Tissue distribution of radioactivity in mice after intravenous injection of [<sup>11</sup>C]MPDX

	% Injection dose/g tissue*					
	1 min	5 min	15 min	30 min	60 min	90 min
Blood	5.23 ± 0.87	3.30 ± 0.03	2.61 ± 0.07	1.78 ± 0.18	1.22 ± 0.19	0.83 ± 0.06
Brain	2.31 ± 0.23	2.53 ± 0.15	1.60 ± 0.07	0.87 ± 0.12	0.46 ± 0.10	0.42 ± 0.08
Heart	4.25 ± 0.48	2.62 ± 0.17	2.00 ± 0.10	1.52 ± 0.13	1.05 ± 0.11	0.74 ± 0.11
Lung	4.55 ± 0.61	3.11 ± 0.04	2.41 ± 0.20	2.04 ± 0.39	1.55 ± 0.26	1.42 ± 0.26
Liver	10.30 ± 1.14	12.14 ± 0.67	11.26 ± 0.45	9.45 ± 1.37	7.52 ± 0.94	4.90 ± 0.25
Spleen	1.71 ± 0.39	1.58 ± 0.04	1.97 ± 0.12	2.52 ± 0.28	3.27 ± 1.24	3.89 ± 0.57
Pancreas	3.58 ± 0.42	2.61 ± 0.13	3.60 ± 0.22	4.33 ± 0.45	5.17 ± 0.70	2.20 ± 0.54
Stomach	1.22 ± 0.47	0.99 ± 0.05	1.27 ± 0.24	1.59 ± 0.67	1.48 ± 0.45	1.31 ± 0.41
Small intestine	2.70 ± 0.45	2.58 ± 0.13	4.12 ± 0.66	7.25 ± 1.04	9.31 ± 1.30	7.17 ± 0.59
Large intestine	1.39 ± 0.31	1.35 ± 0.03	2.20 ± 0.55	1.84 ± 0.23	2.54 ± 0.80	1.61 ± 0.30
Kidney	4.97 ± 0.58	3.85 ± 0.22	3.74 ± 0.32	3.06 ± 0.39	2.41 ± 0.18	1.82 ± 0.12
Testis	1.07 ± 0.38	0.98 ± 0.11	1.97 ± 0.26	1.06 ± 0.15	1.13 ± 0.24	0.48 ± 0.06
Bone	1.69 ± 0.10	1.32 ± 0.25	1.42 ± 0.08	0.79 ± 0.15	0.54 ± 0.08	1.20 ± 0.14
Muscle	0.78 ± 0.14	1.54 ± 0.22	1.15 ± 0.06	1.14 ± 0.14	0.69 ± 0.17	0.42 ± 0.06

\*Mean ± S.D. (n = 4)

**Table 2** Organ distribution of radioactivity in mice after intravenous injection of [<sup>11</sup>C]MPDX

	% Injection dose/organ*					
	1 min	5 min	15 min	30 min	60 min	90 min
Brain	1.11 ± 0.11	1.19 ± 0.04	0.74 ± 0.03	0.40 ± 0.06	0.22 ± 0.05	0.20 ± 0.05
Heart	0.67 ± 0.13	0.41 ± 0.05	0.28 ± 0.01	0.24 ± 0.04	0.16 ± 0.03	0.12 ± 0.02
Lung	1.00 ± 0.12	0.73 ± 0.07	0.48 ± 0.06	0.48 ± 0.13	0.39 ± 0.08	0.35 ± 0.04
Liver	18.09 ± 1.77	22.25 ± 1.61	20.33 ± 1.28	17.03 ± 1.78	12.98 ± 2.57	11.05 ± 0.71
Spleen	0.20 ± 0.05	0.18 ± 0.01	0.26 ± 0.04	0.37 ± 0.10	0.52 ± 0.36	0.41 ± 0.08
Pancreas	0.63 ± 0.06	0.41 ± 0.08	0.51 ± 0.03	0.78 ± 0.08	0.88 ± 0.02	0.75 ± 0.12
Stomach	1.05 ± 0.45	0.75 ± 0.08	0.73 ± 0.08	1.02 ± 0.29	1.17 ± 0.32	0.86 ± 0.27
Small intestine	5.45 ± 1.22	5.50 ± 0.42	6.72 ± 1.98	13.17 ± 1.78	15.99 ± 0.60	17.76 ± 1.32
Large intestine	1.72 ± 0.76	1.48 ± 0.26	3.12 ± 1.44	1.93 ± 0.40	2.96 ± 1.14	2.60 ± 0.23
Kidney	2.52 ± 0.50	2.21 ± 0.20	1.86 ± 0.11	1.51 ± 0.21	1.23 ± 0.28	1.00 ± 0.12
Testis	0.10 ± 0.03	0.07 ± 0.02	0.33 ± 0.03	0.08 ± 0.02	0.10 ± 0.02	0.08 ± 0.02
Bladder	0.03 ± 0.03	0.08 ± 0.04	0.15 ± 0.07	0.10 ± 0.03	0.15 ± 0.14	0.16 ± 0.12
Urine	0.03 ± 0.01	0.24 ± 0.04	2.30 ± 0.33	6.59 ± 1.13	11.04 ± 3.46	10.34 ± 1.91

\*Mean ± S.D. (n = 4)

**Table 3** Absorbed dose of [<sup>11</sup>C]MPDX for human adults estimated from mouse data

	μGy/MBq		μGy/MBq
Brain	0.07	Upper large intestine wall	6.13
Thyroid	3.90	Lower large intestine wall	6.59
Thymus	3.95	Adrenals	4.85
Breast	3.13	Kidneys	2.41
Heart	0.11	Testis	2.87
Lungs	1.43	Ovaries	4.35
Livers	3.26	Uterus	4.40
Pancreas	2.41	Bladder	4.73
Spleen	2.10	Bone surfaces	3.87
Stomach wall	3.07	Red marrow	3.32
Small intestine wall	4.65	Bones	4.21
Total body	3.61 μSV/MBq		

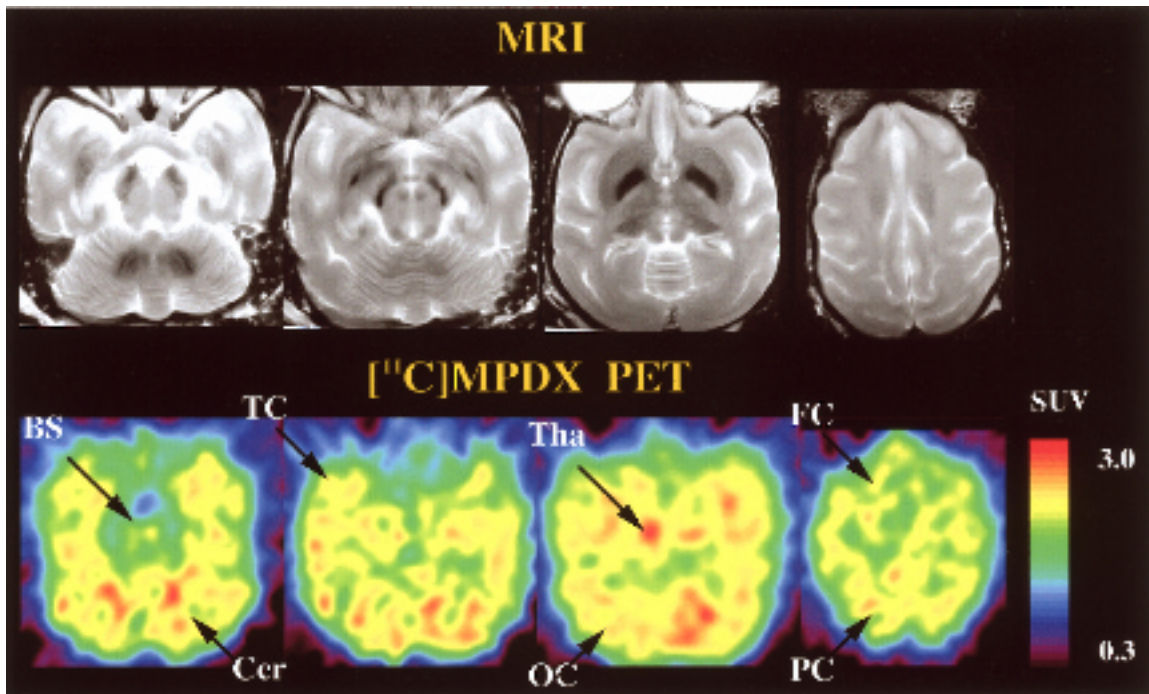


**Fig. 2** Brain images of the monkey by PET with [ $^{11}\text{C}$ ]MPDX (lower line) and a standard MRI of the corresponding slices (upper line). The PET images were acquired from 30 to 60 min after injection. The range of radioactivity level was 3.0–0.3 SUV.

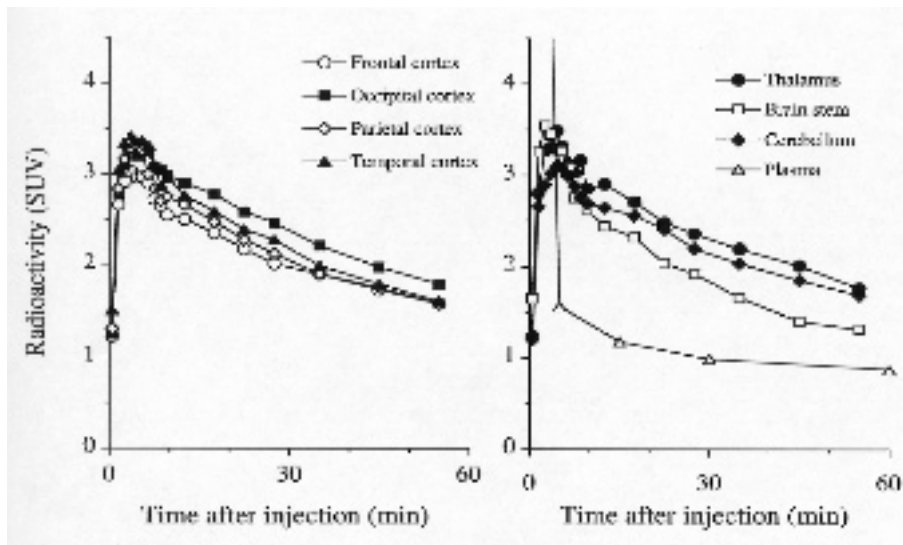


**Fig. 3** Time-radioactivity curves of the seven brain regions and plasma after intravenous injection of [ $^{11}\text{C}$ ]MPDX into a monkey. The radioactivity levels are expressed as the SUV.

was assessed as the SUV and the labeled metabolites were analyzed as previously described.<sup>16</sup>

## RESULTS

### Radiation dosimetry

The tissue distribution of the radioactivity after injection of [ $^{11}\text{C}$ ]MPDX into mice is summarized in Tables 1 and

2. The liver showed the highest initial uptake (%ID/g) followed by the kidneys, lungs, heart, pancreas, small intestines and brain. The level of radioactivity in the liver increased for the first 5 min and then gradually decreased. The levels in the kidneys, lungs, heart, brain and blood gradually decreased, whereas those in the pancreas and small intestines increased for 60 min and then decreased. The levels in other tissues investigated were low. From

these data, the radiation-absorbed doses were estimated (Table 3). The radiation-absorbed doses were slightly higher in the upper and lower large intestine walls than in the other organs studied, and were very low in the brain and heart.

#### *Acute toxicity*

Acute toxicity was evaluated after an intraperitoneally single administration of MPDX at a dose of 3.73 mg/kg, and after an intravenous injection of three lots of [<sup>11</sup>C]MPDX preparations in a dose range of 1.43–5.71 µg/kg. No mortality was found in the rats. All groups of rats showed normal gain in body weight compared with the control animals, and any no clinical signs were observed over a 15-day period. Also no abnormality was found in their postmortem macroscopic examination.

#### *Mutagenicity*

When a bacterial reverse mutation test was conducted on *Salmonella typhimurium* mutation test, no mutagenic activity was observed for MPDX.

#### *PET imaging of adenosine A<sub>1</sub> receptors in the monkey brain*

Figure 2 shows the PET brain images of [<sup>11</sup>C]MPDX in the monkey. The tracer was widely distributed in all brain regions. Figure 3 shows the time-activity curves of [<sup>11</sup>C]MPDX in the seven brain regions and plasma. The radioactivity level of [<sup>11</sup>C]MPDX reached maximal at 5 min and then decreased. Plasma radioactivity rapidly decreased after a bolus injection of each of the two tracers. Percentages of the unchanged form of radioligand rapidly decreased: 78%, 70%, 54% and 41%, at 5, 15, 30 and 60 min, respectively (n = 2).

## DISCUSSION

In previous *in vivo* studies on mice, rats and cats, we have demonstrated that [<sup>11</sup>C]MPDX has the potential for mapping adenosine A<sub>1</sub> receptors in the CNS as a PET ligand as its propylated analog [<sup>11</sup>C]KF15372.<sup>15–18</sup> In the present work, we investigated the dosimetry of [<sup>11</sup>C]MPDX and the acute toxicity and mutagenicity of MPDX as a pre-clinical study. We also performed PET imaging of the monkey brain.

The radiation absorbed-dose was slightly higher in the large intestine wall than in other organs studied, but was low enough for clinical use. No abnormality in rats in the acute toxicity test and no mutagenicity of MPDX demonstrate the clinical suitability of [<sup>11</sup>C]MPDX in PET studies of humans.

In the monkey brain, the regional distribution pattern of [<sup>11</sup>C]MPDX was similar to that of [<sup>11</sup>C]KF15372. Although the receptor-specific binding of [<sup>11</sup>C]MPDX was not investigated by the receptor blockade in the present study, that of [<sup>11</sup>C]KF15372 was clearly demonstrated

in the previous study.<sup>17</sup> In the monkey brain, more [<sup>11</sup>C]MPDX was taken up by the brain and was washed out faster than [<sup>11</sup>C]KF15372,<sup>17</sup> reflecting their *in vitro* affinities for the adenosine A<sub>1</sub> receptors: K<sub>i</sub> = 4.2 nM for [<sup>11</sup>C]MPDX and K<sub>i</sub> = 3.0 nM for [<sup>11</sup>C]KF15372.<sup>16</sup> Similar time-activity curve patterns were also observed in the cat brain.<sup>18</sup>

Previous work has established a role for adenosine in a diverse array of neural phenomena, which include regulation of sleep and the level of arousal, neuroprotection, regulation of seizure susceptibility, locomotor effects, analgesia, mediation of the effects of ethanol and chronic drug use.<sup>5</sup> Therefore, interaction with adenosine metabolism is a promising target for therapeutic intervention in ischemic brain disorders, neurological and psychiatric diseases such as epilepsy, sleep, movement (parkinsonism or Huntington's disease) or psychiatric disorders (Alzheimer's disease, depression, schizophrenia or addiction).<sup>4,6</sup> In the studies on the post-mortem human brain, a reduced density of adenosine A<sub>1</sub> receptors was found in the hippocampus of patients with Alzheimer's disease.<sup>27,28</sup> Angelatou et al.<sup>29</sup> detected a significant increase in adenosine A<sub>1</sub> receptor binding in the neocortex obtained from patients suffering from temporal lobe epilepsy. The [<sup>11</sup>C]MPDX PET is of interest in diagnosing patients suffering from epilepsy to understand the pathogenesis of epilepsy and of patients with other neurological and psychiatric diseases.

In conclusion, these pieces of evidence demonstrated that [<sup>11</sup>C]MPDX is suitable for mapping adenosine A<sub>1</sub> receptors in the human brain by PET.

## ACKNOWLEDGMENTS

This work was supported by a Grant-in-Aid for Scientific Research (C) No. 10670883 from the Ministry of Education, Culture, Sports, Science and Technology, Japan.

## REFERENCES

1. Fredholm BB, Abbracchio MP, Burnstock G, Daly JW, Harden TK, Jacobson KA, et al. Nomenclature and classification of purinoceptors. *Pharmacol Rev* 1994; 46: 143–156.
2. Palmer TM, Stiles GL. Adenosine receptors. *Neuropharmacology* 1995; 34: 683–694.
3. Ongini E, Fredholm BB. Pharmacology of adenosine A<sub>2A</sub> receptors. *Trends Pharmacol Sci* 1996; 17: 364–372.
4. Haas HL, Selbach O. Functions of neuronal adenosine receptors. *Naunyn Schmiedebergs Arch Pharmacol* 2000; 362: 375–381.
5. Dunwiddie TV, Masino SA. The role and regulation of adenosine in the central nervous system. *Ann Rev Neurosci* 2001; 24: 31–55.
6. von Lubitz DK. Adenosine in the treatment of stroke: yes, maybe, or absolutely not? *Expert Opin Investig Drugs* 2001; 10: 619–632.
7. Lewis ME, Patel J, Moon Edley S, Marangos PJ. Autora-

- diographic visualization of rat brain adenosine receptors using  $N^6$ -cyclohexyl[ $^3\text{H}$ ]adenosine. *Eur J Pharmacol* 1981; 73: 109–110.
8. Goodman RR, Snyder SH. Autoradiographic localization of adenosine receptors in rat brain using [ $^3\text{H}$ ]cyclohexyladenosine. *J Neurosci* 1982; 2: 1230–1241.
  9. Fastbom J, Pazos A, Palacios JM. The distribution of adenosine A<sub>1</sub> receptors and 5'-nucleotidase in the brain of some commonly used experimental animals. *Neuroscience* 1987; 22: 813–826.
  10. Fastbom J, Pazos A, Probst A, Palacios JM. Adenosine A<sub>1</sub> receptors in the human brain: a quantitative autoradiographic study. *Neuroscience* 1987; 22: 827–839.
  11. Svenningsson P, Hall H, Sedvall G, Fredholm BB. Distribution of adenosine receptors in the postmortem human brain: an extended autoradiographic study. *Synapse* 1997; 27: 322–335.
  12. Schindler M, Harris CA, Hayes B, Papotti M, Humphrey PP. Immunohistochemical localization of adenosine A<sub>1</sub> receptors in human brain regions. *Neurosci Lett* 2001; 297: 211–215.
  13. Mally J, Stone TW. Potential role of adenosine antagonist therapy in pathological tremor disorders. *Pharmacol Ther* 1996; 72: 243–250.
  14. Ishiwata K, Furuta R, Shimada J, Ishii S, Endo K, Suzuki F, et al. Synthesis and preliminary evaluation of [ $^{11}\text{C}$ ]KF15372, a selective adenosine A<sub>1</sub> antagonist. *Appl Radiat Isot* 1995; 46: 1009–1013.
  15. Furuta R, Ishiwata K, Kiyosawa M, Ishii S, Saito N, Shimada J, et al. Carbon-11 labeled KF15372: a potential central nervous system adenosine A<sub>1</sub> receptor ligand. *J Nucl Med* 1996; 37: 1203–1207.
  16. Noguchi J, Ishiwata K, Furuta R, Shimada J, Kiyosawa M, Ishii S, et al. Evaluation of carbon-11 labeled KF15372 and its ethyl and methyl derivatives as a potential CNS adenosine A<sub>1</sub> receptor ligand. *Nucl Med Biol* 1997; 24: 53–59.
  17. Wakabayashi S, Nariai T, Ishiwata K, Nagaoka T, Hirakawa K, Oda K, et al. A PET study of adenosine A<sub>1</sub> receptor in anesthetized monkey brain. *Nucl Med Biol* 2000; 27: 401–406.
  18. Shimada Y, Ishiwata K, Kiyosawa M, Nariai T, Oda K, Toyama H, et al. Mapping adenosine A<sub>1</sub> receptors in the cat brain by positron emission tomography with [ $^{11}\text{C}$ ]MPDX. *Nucl Med Biol* 2002; 29: 29–37.
  19. Kiyosawa M, Ishiwata K, Noguchi J, Endo K, Wang WF, Suzuki F, et al. Neuroreceptor bindings and synaptic activity in visual system of monocularly enucleated rat. *Jpn J Ophthalmol* 2001; 45: 264–269.
  20. Shimada Y, Nariai T, Ishiwata K, Ishii S, Oda K, Ando M, et al. Decrease in adenosine A<sub>1</sub> receptor binding potential after reperfusion as a predictor of severe cerebral ischemic insult—PET multitracer study in cats' model of transient MCA occlusion. *J Cereb Blood Flow Metab* 1999; 19: S249.
  21. Shimada J, Suzuki F, Nonaka H, Karasawa A, Mizumoto H, Ohno T, et al. 8-(Dicyclopropylmethyl)-1,3-dispropylxanthine: a potent and selective adenosine A<sub>1</sub> antagonist with renal protective and diuretic activities. *J Med Chem* 1991; 34: 466–469.
  22. Suzuki F, Shimada J, Mizumoto H, Karasawa A, Kubo K, Nonaka H, et al. Adenosine A<sub>1</sub> antagonists. 2. Structure-activity relationships on diuretic activities and protective effects against acute renal failure. *J Med Chem* 1992; 35: 3066–3075.
  23. Suzuki F, Shimada J, Shiozaki S, Ichikawa S, Ishii A, Nakamura J, et al. Adenosine A<sub>1</sub> antagonists. 3. Structure-activity relationships on amelioration against scopolamine- or  $N^6$ -(*R*-phenylisopropyl)adenosine-induced cognitive disturbance. *J Med Chem* 1993; 36: 2508–2518.
  24. Ishiwata K, Ido T, Mejia AA, Ichihashi M, Mishima Y. Synthesis and radiation dosimetry of 4-boron-2-[ $^{18}\text{F}$ ]fluoro-D,L-phenylalanine: A target compound for PET and boron neutron capture therapy. *Appl Radiat Isot* 1991; 142: 325–328.
  25. Mejia AA, Nakamura T, Itoh M, Hatazawa J, Ishiwata K, Ido T, et al. Absorbed dose estimates in positron emission tomography studies based on the administration of  $^{18}\text{F}$ -labeled radiopharmaceuticals. *J Radiat Res* 1991; 32: 243–261.
  26. Watanabe M, Uchida H, Okada H, Shimizu K, Satoh N, Yoshikawa E, et al. A high resolution PET for animal studies. *IEEE Trans Med Imag* 1992; 11: 577–580.
  27. Jansen K, Faull RLM, Dragunow M, Synek BJL. Alzheimer's disease: changes in hippocampal *N*-methyl-D-aspartate, quisqualate, neurotensin, adenosine, benzodiazepine, serotonin and opioid receptors—an autoradiographic study. *Neuroscience* 1990; 39: 613–627.
  28. Ulas J, Brunner LC, Nguyen L, Cotman CW. Reduced density of adenosine A<sub>1</sub> receptors and preserved coupling of adenosine A<sub>1</sub> receptors to G proteins in Alzheimer hippocampus: a quantitative autoradiographic study. *Neuroscience* 1993; 52: 843–854.
  29. Angelatou F, Pagonopoulou O, Maraziotis T, Olivier A, Villemeure JG, Avoli M, et al. Upregulation of A<sub>1</sub> adenosine receptors in human temporal lobe epilepsy: a quantitative autoradiographic study. *Neurosci Lett* 1993; 163: 11–14.